

FUNCTIONAL PARAMETERS OF SENSORS FOR THE EXTENDED CROSS-FLOAT METHOD

Adam Brzozowski^{1,2)}, Roman Szewczyk³⁾, Piotr Gazda¹⁾, Michał Nowicki⁴⁾

1) *Institute of Metrology and Measuring Systems, Faculty of Mechatronics, Warsaw University of Technology, sw. A. Boboli 8, 02-525 Warsaw, Poland*

2) *Central Office of Measures, Elektoralna 2, 00-139 Warsaw, Poland*

3) *Lukasiewicz Research Network – Industrial Research Institute for Automation and Measurements PIAP, Al. Jerozolimskie 202; 02-486 Warsaw, Poland (✉ roman.szewczyk@piap.lukasiewicz.gov.pl)*

4) *Department of Mechatronics, Robotics and Digital Manufacturing, Faculty of Mechanics, Vilnius Gediminas Technical University, Plytinės g. 25, LT-10105 Vilnius, Lithuania*

Abstract

This study enables the justified selection of suitable sensors for the extended cross-float method for the calibration of piston gauges. Three sensor types were tested: a triangulation laser sensor, a capacitive sensor, and a high-precision accelerometer. The extended cross-float method is employed to avoid determining the equilibrium point between interconnected manometers during piston gauge calibration, assessing the fall rate and displacement of the piston. Thus, this makes the above parameters the most relevant and crucial for the mentioned method. The performance of each sensor was evaluated under identical load-pressure conditions to ascertain their accuracy in measuring piston displacement and fall rate. The laser sensor demonstrated the highest measurement precision, while the capacitive sensor effectively smoothed data, mitigating the impact of surface irregularities. Despite its ease of use and installation, the accelerometer showed notable data noise and less accurate results than the other sensors. These findings provide a comparative analysis of sensor performance, highlighting their respective advantages and limitations in the context of high-precision pressure measurement applications.

Keywords: piston gauge, dead-weight tester, extended cross-float, fall rate, pressure calibration.

1. Introduction

The advancements in manufacturing technology and production capabilities have ensured that, despite the concept of the piston-cylinder gauge being over 150 years old, modern implementations of these instruments offer excellent measurement accuracy with very low uncertainties [1]. These qualities are highly sought after in various applications within the field of metrology. For instance, the redefinition of the Boltzmann constant, one of the key parameters used in temperature analysis, exemplifies such applications [2], [3]. The determination of the effective cross-sectional area of high-accuracy measurement assemblies is often conducted using analytical methods based on geometric measurements of the piston and corresponding sleeve [4]. However, this method is not suitable for assemblies with smaller cross-sections, and its use is not economically or substantively justified for assemblies of lower accuracy classes, which are increasingly prevalent in accredited calibration laboratories. In such cases, the cross-float method, either in manual or automated form, is most commonly employed [5]. It is worth noting that this area of metrology represents a scope of demand for pressure measurements in numerous industries, such as the automotive, heavy industry, energy, and fuel sectors, as well as the armaments. These industries, with an annual total turnover of over 180 billion USD, await rapid, precise, and reliable calibration of measuring instruments used in their laboratories.

The practical aim of the cross-float measurement method applied in the calibration of piston gauges is to determine the equilibrium point of two interconnected manometers with their pistons in operational position [6]. The measurement point is defined as the moment when both the reference device and the calibrated device descend steadily at their nominal piston fall rate [7]. From the perspective of practical metrological work, it is also crucial to consider the vicinity of the precise measurement point. An accurate examination of the measurement system's behavior in the case of imbalance [8] can be utilized to conduct a dynamic analysis, providing an approximate value of the mass that should be added or removed to achieve equilibrium [9]. The piston fall rate parameter is dependent on several factors - initially, the most important ones are the dimensions of the piston and cylinder, but the material used to make the measurement system also plays a significant role, as it affects the piston's reaction to the applied pressure. Additionally, the quality of the measurement system's execution, including shape errors and surface finishing quality, also has an impact. All these elements are reflected in the fall rate, which is why its precise determination is crucial in dynamic measurements. The piston's movement rate is influenced by various factors, including:

- the size and shape of the piston and cylinder,
- the material used to make the measurement system,
- the quality of the system's construction, including any potential shape errors or surface finish issues.

These factors all contribute to the overall fall rate, which is critical to measure accurately in dynamic conditions. This study aims to compare, in the above context, three different methods of piston fall rate measurements [10] – using a triangulation laser sensor, a capacitive sensor, and an accelerometer. These methods have an established and well-recognized operational methodology, and their specifications are known in general applications. However, they have not been thoroughly investigated in such a specialized and narrow application as the measurement of piston fall rate. The aim of this study is to experimentally verify the influence of the characteristics of these three types of sensors in practical application, specifically in the context of dead-weight piston gauges. Particularly interesting will be the inclusion of the accelerometric sensor in the comparison, as this type of measuring instrument is not typically used in the calibration of dead-weight piston gauges. In the standard cross-float method, the desired measurement point is characterized by motion without acceleration. Hence, the application of this type of sensor only makes sense in the extended cross-float method.

2. State of the Art

In the context of a piston gauge, "fall rate" refers to the rate at which the piston descends due to the combined effects of the applied load (pressure) and the system's characteristics [11]. The fall rate is a critical parameter as it can affect the accuracy and stability of the pressure measurement [12].

Measurement of displacement is one of the most well-recognized areas in metrology due to its high frequency of application in industrial, manufacturing, and broadly understood commercial solutions [13], [14]. There are numerous methods for measuring distance, each with its strengths and weaknesses that must be considered in the context of specific requirements regarding measurement range, accuracy, repeatability, as well as defined technical solutions or individual technological needs. One such requirement, in the context of fall rate measurements, is the necessity to maintain a non-contact measurement principle to avoid undefined additional influences on the primary load's reference mass. For this reason, it is impossible to use popular and reliable solutions such as various linear encoders or classical dial gauges. Among non-contact displacement measurement methods, the most popular are those

utilizing, among others, laser sensors, optical sensors, ultrasonic sensors, capacitive sensors, inductive sensors, and magnetic sensors [15].

Typically, triangulation laser sensors are the most commonly used for determining piston velocity [16]. Alternatively, one may encounter other methods, such as visual methods utilizing digital optical cameras [17]. However, it is essential to emphasize that these solutions are applied to observe piston fall rate at a constant velocity. Situations, where the fall rate is taken with its dynamic, varies are not taken into account, and consequently, this phenomenon is not considered in the mathematical calculations for determining the effective cross-sectional area of the calibrated manometer piston effective area. The extended cross-float method could reduce the time required for conducting measurements in the calibration of piston pressure gauges. Moreover, decreasing the labor intensity will contribute to disseminating and popularizing this method among calibration laboratories accredited in the pressure field.

3. Methodology

To conduct a comparison of sensors, a measurement setup was prepared consisting of two interconnected reference instruments, MTU-6, with a measurement range of (0.02 - 6) bar, which is presented in Fig. 1. Positioned between them was a valve allowing the separation of the measuring instruments into individual pressure systems [18]. Opening the valve resulted in the rapid connection of the pressure systems, causing displacement of the pistons in the measuring assemblies [19]. All three sensors were placed under the same load-pressure conditions, which can be seen in Fig. 2 and the same piston displacement velocity changes were observed. The list of sensors used in the study is provided in Table 1. All applied methods featured non-contact measurement, ensuring uninterrupted operation of the measuring assemblies. However, it should be noted that to maximize functionality and minimize errors associated with sensor mounting reconfiguration, the mounting position was selected under the first reference mass. This allowed for the investigation of various measurement points within the measurement range without the need for physical modification of the test setup. Naturally, the consequence of moving the displacement sensor measurement point away from the piston rotation axis is an increased reading spread due to errors caused by the shape of the reference weights. Nevertheless, software-based mitigation of adverse effects through signal analysis is feasible, considering the high data acquisition frequency and the overall repeatability of observed fluctuations. In contrast, regarding the acceleration sensor, the situation is quite different. Due to its wireless design, in most cases, it can be placed directly on the piston rotation axis without the need for displacement during subsequent measurement points. Of course, with specific designs, removal of the acceleration sensor may be necessary before applying reference masses [20]. However, even in this scenario, its reinstallation is straightforward and not burdened with additional potential errors related to position changes.

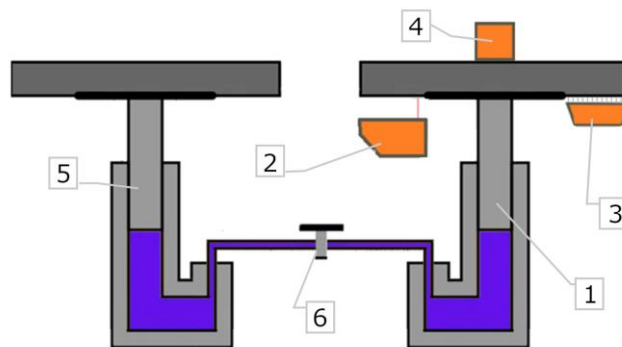


Fig. 1. Schematic diagram of the test stand for the fall rate dynamic change measurements: 1 – pressure balance under test, 2 - laser sensor, 3 – capacity sensor, 4 – accelerometer, 5 - reference instrument, 6 – separating valve.

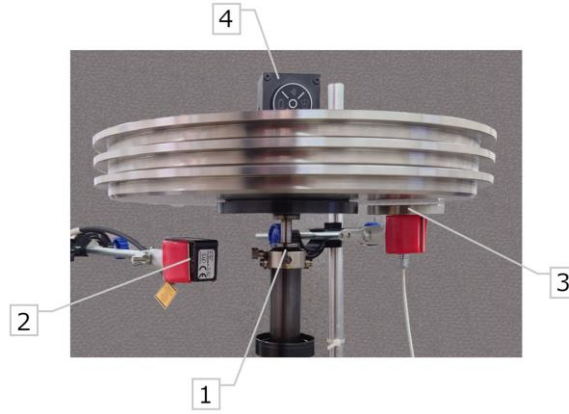


Fig. 2. Sensor setup close-up: 1 – pressure balance under test, 2 – laser sensor, 3 – capacity sensor, 4 – accelerometer.

Table 1. Sensors used in measurements with measurement ranges.

| Sensor type | Manufacturer | Sensor name | Operating range |
|---------------|---------------|-------------|-----------------|
| Accelerometer | Alitec | CI@ve | ± 16 g |
| Laser | Micro-Epsilon | ILD1420-25 | (0 – 25) mm |
| Capacity | Micro-Epsilon | NCDT6200 | (0 – 20) mm |

4. Results

The obtained numerical data had to be transformed due to the nature of the measurement results from individual sensors. The laser sensor and the capacitive sensor measured displacement directly; thus, the piston fall rate was obtained by calculating the time derivative. On the other hand, the results from the accelerometer concerned acceleration (a), so the piston fall rate (v) was obtained by performing integration over time (t) in the range ($b \div c$). Because of oversampling, a Riemann sum was used for numerical integration:

$$v(t) = \int_b^c f(a)dt = \lim_{n \rightarrow \infty} \sum_{i=0}^{n-1} f(a_i)\Delta t \quad (1)$$

Further integration allowed for the determination of the piston displacement (s):

$$s(t) = \int_b^c f(v)dt = \lim_{n \rightarrow \infty} \sum_{i=0}^{n-1} f(v_i)\Delta t \quad (2)$$

These mathematical operations made it possible to compare the obtained results. It is important to note that a key issue was the standardization of the time measurement parameter. Due to delays in non-integrated data recording systems, correcting the data based on observed phenomena was necessary. It is also worth mentioning that the accelerometer had the best data collection frequency at the level of 32 Hz, while the laser sensor and the capacitive sensor provided a frequency at the level of 4 Hz.

The final results are presented in the Fig. 3 and Fig. 4:

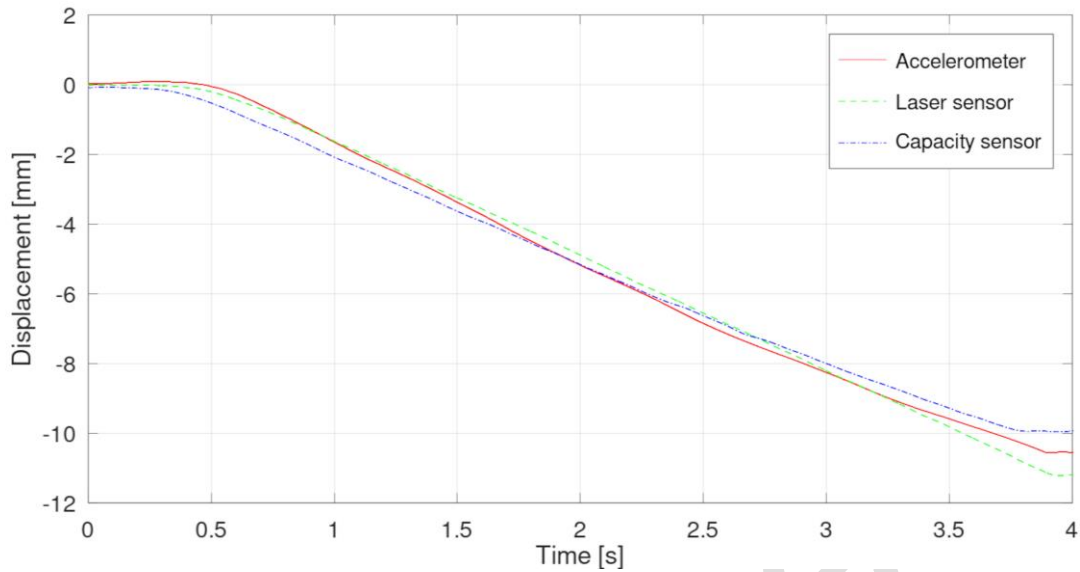


Fig. 3. Comparison of displacement data gathered by accelerometer, laser sensor and capacity sensor.

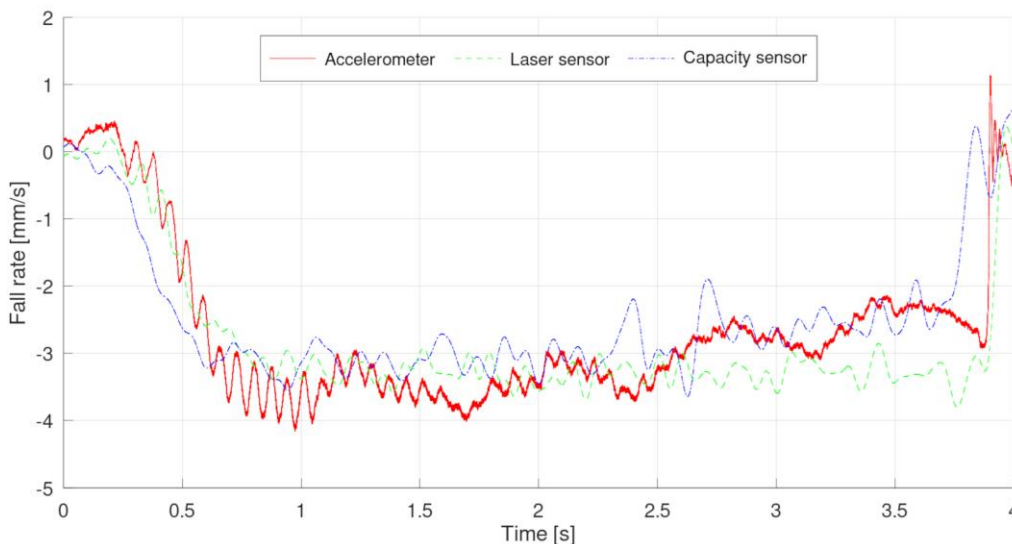


Fig. 4. Comparison of fall rate data gathered by an accelerometer, laser sensor, and capacity sensor.

The obtained results were reasonably consistent, although they exhibited some crucial differences among utilized sensors. One of the most critical aspects was identifying a common starting point for observations – the reaction time to changes varied among the sensors, complicating this issue. It is important to note that not all configuration elements were optimal due to the nature of the measurements and the installation method. For example, due to the rotational motion of the piston and the reference masses, grounding the measured object, which is recommended by the capacitive sensor manufacturer, was impossible. Furthermore, appropriate calibration and adjustment of the sensors are vital, as even minor shifts in their characteristics can result in significant inaccuracies in the final measurement results. This is particularly evident in the case of the accelerometer due to the numerical computation methods employed to derive the displacement parameter from the measured acceleration [21].

However, evaluating the obtained results through the prism of the assumed future purpose is indispensable, namely, to use them in the extended cross-float method. Thus, it is necessary

to assess the value of the achieved results in the context of the need to analyze a specific part of them, representing the free displacement of the pistons of the measuring units connected through the pressure transfer medium. Due to the nature of the physical phenomenon, the expected characteristics of the changes should be linear, as can be seen in Fig. 5, so the observed trend line should be evaluated against the conformity to a linear function.

For this purpose, the *root mean square error* (RMSE) has been calculated by taking into account values predicted by the linear regression (s_l) and measured values (s_i) as:

$$RMSE = \sqrt{\frac{\sum_{i=1}^n (s_l - s_i)^2}{n}} \quad (3)$$

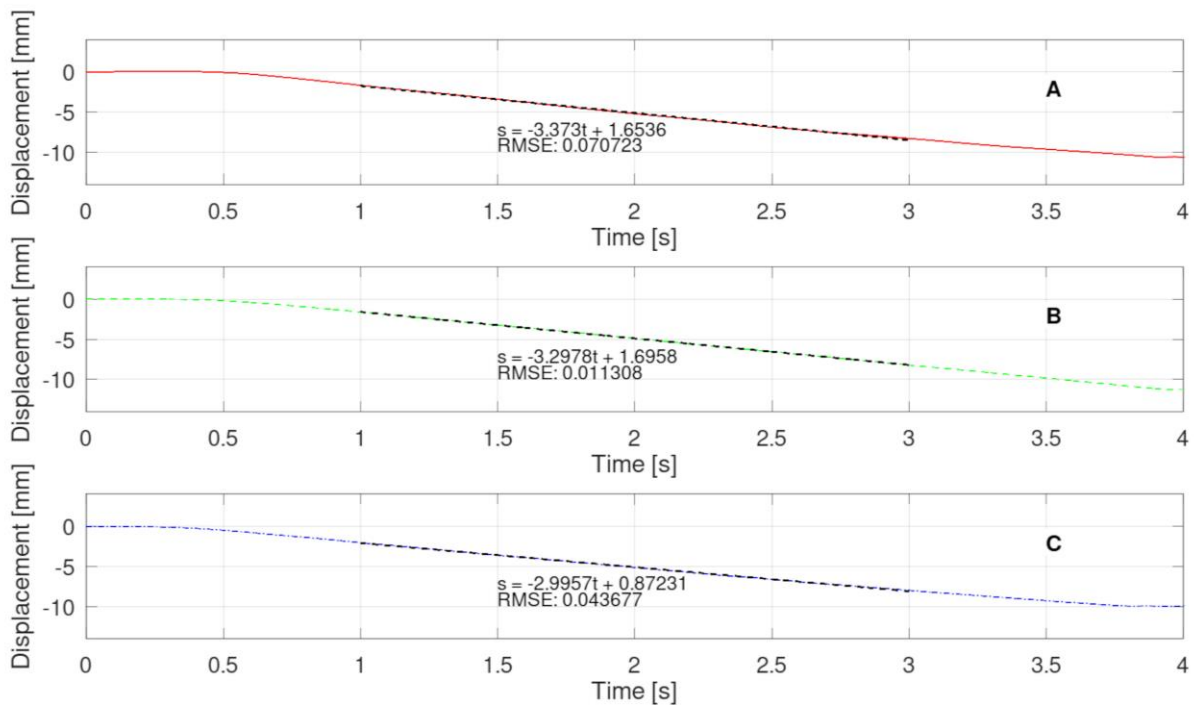


Fig. 5. Trend lines computed for every sensor's characteristics (displacement): A – accelerometer, B – laser sensor, C – capacity sensor.

Similar calculations were performed for the obtained piston fall rates. As a result, the piston fall rate was calculated from the data set during the fall, which is shown in the Fig. 6. Moreover, the information about the time drift of the sensor can be estimated from the value of the multiplicative factor in the linear regression.

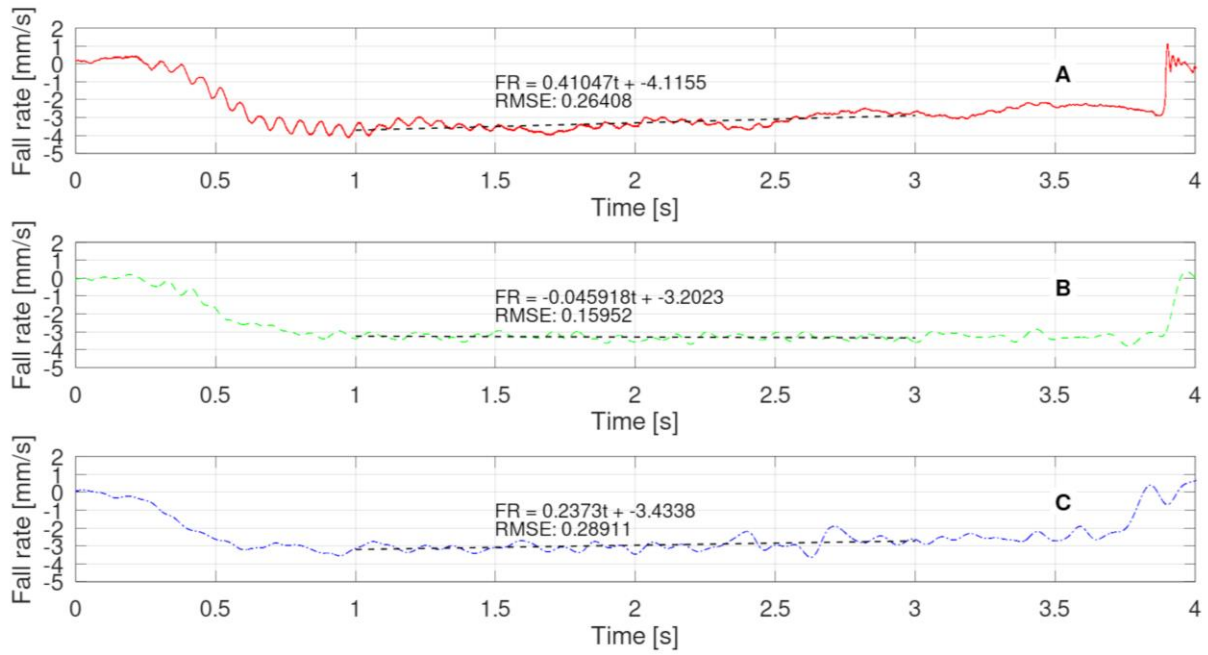


Fig. 6. Trend lines computed for every sensor's characteristics (fall rate): A – accelerometer, B – laser sensor, C – capacity sensor.

Table 2. Results of RMSE factor for displacement and fall rate for different sensors.

| Plot | Sensor type | Dynamic displacement measurement RMSE value (mm) | Fall rate (mm/s) | Fall rate RMSE value (mm/s) |
|------|---------------|--|------------------|-----------------------------|
| A | Accelerometer | 0.071 | 4.12 | 0.264 |
| B | Laser | 0.011 | 3.20 | 0.159 |
| C | Capacity | 0.044 | 3.43 | 0.289 |

Table 3. Standard deviation estimation calculated for the coefficients determining trend lines.

| Plot | Sensor type | Standard deviation estimator | |
|------|---------------|------------------------------|---------------------|
| | | Slope | Interception |
| A | Accelerometer | $4.7 \cdot 10^{-4}$ | $9.9 \cdot 10^{-4}$ |
| B | Laser | $2.2 \cdot 10^{-4}$ | $4.6 \cdot 10^{-4}$ |
| C | Capacity | $8.6 \cdot 10^{-4}$ | $1.8 \cdot 10^{-3}$ |

The RMSE for the linear approximation clearly indicates that the best fit can be observed for measurements using a laser sensor, as indicated by the results summarized in Table 2, whereas the assessment of the uncertainty of the linear regression is given in Table 3. The second best fit turned out to be measurements using a capacitive sensor. By far, the least good fit in this context turned out to be measurements obtained with an accelerometer. It's worth noting that the higher degree of polynomial regression did not enhance the fitting quality. An analysis of potential influencing factors is illustrated in Fig. 7.

A similar conclusion can be drawn from the analysis based on the standard deviation calculated for the coefficients of the obtained trend lines, with data presented in Table 3. According to this criterion, the data collected using the laser sensor exhibited the greatest consistency and the smallest dispersion. The accelerometer ranked second in terms of quality in this category, while the capacitive sensor performed the worst.

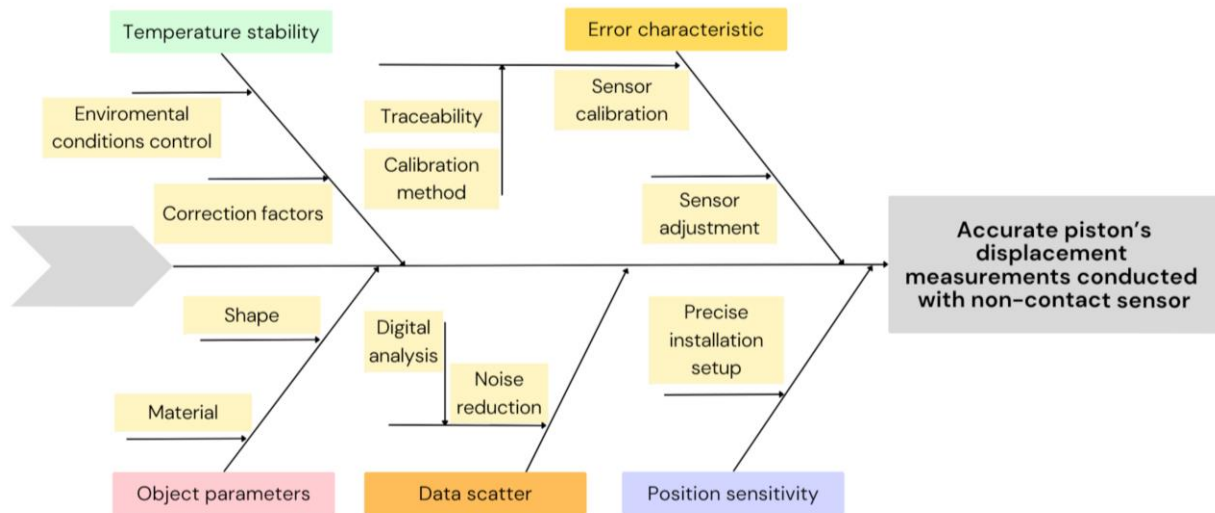


Fig. 7. Factors affecting the quality of non-contact displacement measurements.

Each sensor can be evaluated within each category mentioned in Fig. 7. The results of this comparison are presented in Table 4. A higher grade means the sensor has better abilities in a certain category than others.

Table 4. Sensors functional properties evaluation.

| Sensor type \ Category | Temperature Stability | Error Characteristic | Data scatter | Position sensitivity |
|------------------------|-----------------------|----------------------|--------------|----------------------|
| Accelerometer | + | + | ++ | +++ |
| Laser | ++ | ++ | +++ | + |
| Capacity | +++ | ++ | + | + |

5. Conclusions

The analysis of the results clearly highlighted the strengths and weaknesses of each tested measurement solution for extended cross-float measurements. The laser sensor demonstrated the highest measurement precision in this context, which simultaneously accentuated the imperfections in constructing the reference weights. Due to its design, the capacitive sensor naturally smoothed the collected data, thereby reducing the significance of surface irregularities on the reference plane. However, its dimensions, physical size, and measurement field conditions make it impractical for universal application with every weight-loaded piston manometer. For low measurement ranges (especially with gaseous pressure media) and unconventional instrument constructions, the use of this sensor may be impossible. On the other hand, the accelerometer sensor is characterized by excellent functionality and unparalleled ease of use and installation. Unfortunately, the level of data noise and the significant influence of the initial state on the final calculations means that the results obtained are far from reality and only provide a rough approximation of the actual behavior observed in the measured assembly of the weight-loaded piston manometer.

The adopted computational rules and the results obtained based on the input data clearly indicate that the best choice for applying the extended cross-float method will be a laser sensor - in this case, the RMSE values were smaller by an average of over 1.6 times compared to the accelerometer and 1.8 times compared to the capacitive sensor in terms of the measured fall rate. This is also indicated by the comparison of the calculation results for displacement, where the laser sensor showed 6.4 times better results than those of the accelerometer and four times better results than those of the capacitive sensor.

As part of the further development of the measurement setup for piston fall rate measurement and for the purpose of an in-depth comparative analysis of the aforementioned sensors, it is worth considering the idea of using a stepper motor as auxiliary equipment. Such a solution would allow independence from the varied initial conditions dependent on the operator; however, it should be noted that its practical implementation would be possible only under specific conditions dictated by the design solutions employed by the manufacturers of the piston gauges.

Acknowledgments

The work was created as a result of the implementation of the "Implementation Doctorate" program financed by the Ministry of Education and Science.

References

- [1] Sabuga, W. (2024). Recent research results on piston gauges. *Proceedings of the 7th IMEKO TC16 Conference on Pressure and Vacuum Measurement*, 1–6. <https://doi.org/10.21014/tc16-2023.11>
- [2] Fischer, J., Fellmuth, B., Gaiser, C., Zandt, T., Pitre, L., Sparasci, F., Plimmer, M. D., de Podesta, M., Underwood, R., Sutton, G., Machin, G., Gavioso, R. M., Madonna Ripa, D., Steur, P. P. M., Qu, J., Feng, X. J., Zhang, J., Moldover, M. R., Benz, S. P., ... del Campo, D. (2018). The Boltzmann project. *Metrologia*, 55(2), R1–R20. <https://doi.org/10.1088/1681-7575/aaa790>
- [3] Sabuga, W., Priuenrom, T., Haines, R., & Bair, M. (2011). *Design and Evaluation of Pressure Balances with $1 \cdot 10^{-6}$ Uncertainty for the Boltzmann Constant Project*. PTB Mitteilungen, 121(3), 256–259.
- [4] Jusko, O., Bastam, D., Neugebauer, M., Reimann, H., Sabuga, W., & Priuenrom, T. (2010). Final Results of the Geometrical Calibration of the Pressure Balances to be Used for the new Determination of the Boltzmann Constant. *Key Engineering Materials*, 437, 150–154. <https://doi.org/10.4028/www.scientific.net/kem.437.150>
- [5] Y. Yang, R.G. Driver, J.S. Quintavalle, J. Scherschligt, K. Schlatter, J.E. Ricker, G.F. Strouse, D.A. Olson, J.H. Hendricks, *An integrated and automated calibration system for pneumatic piston gauges*. Measurement 134, 1–5 (2019). <https://www.doi.org/10.1016/j.measurement.2018.10.050>
- [6] Hamarat, A., Yilmaz, R., Durgut, Y., & Demir, E. (2023). Calibration of pressure balances. *AIP Conference Proceedings*, 2803, 030006. <https://doi.org/10.1063/5.0143464>
- [7] Kajikawa, H., Ide, K., & Kobata, T. (2011). Method for altering deformational characteristics of controlled-clearance piston-cylinders. *Measurement*, 44(2), 359–364. <https://doi.org/10.1016/j.measurement.2010.10.011>
- [8] Kumar, R., Yadav, K., Dubey, P. K., Zafer, A., Kumar, A., & Yadav, S. (2024). Design, Development, and Analysis of Ultrasonic Fall Rate Measuring System for Primary Pressure Standard. *Journal of The Institution of Engineers (India): Series C*, 105(1), 31–39. <https://doi.org/10.1007/s40032-023-01019-7>
- [9] Simpson, D. I. (1994). Computerized Techniques for Calibrating Pressure Balances. *Metrologia*, 30(6), 655–658. <https://doi.org/10.1088/0026-1394/30/6/021>
- [10] Brzozowski, A., Szewczyk, R., Gazda, P. & Nowicki, M. (2023). *The Measurement Method of a Piston Fall Rate*. *Pomiary Automatyka Robotyka*, 4(27), 65–69. https://www.doi.org/10.14313/PAR_250/65
- [11] Durgut, Y. (2022). Metrological characterisation of force-balanced piston gauge up to 15,000 Pa pressure range. *MAPAN*, 38(1), 147–159. <https://doi.org/10.1007/s12647-022-00586-x>
- [12] Thakur, V. N., Sharma, R., Kumar, H., Omprakash, Vijayakumar, D. A., Yadav, S., & Kumar, A. (2020). On long-term stability of an air piston gauge maintained at National Physical Laboratory, India. *Vacuum*, 176, 109357. <https://doi.org/10.1016/j.vacuum.2020.109357>
- [13] Xu, P., Li, R. J., Zhao, W. K., Chang, Z. X., Ma, S. H., & Fan, K. C. (2021). Development and verification of a high-precision laser measurement system for straightness and parallelism measurement. *Metrology and Measurement Systems*, 479–495. <https://doi.org/10.24425/mms.2021.137132>

- [14] Yinggang, Z., Shanhui, W., Guangping, Y., & Zhou, Y. (2010). Capacitive sensor high-precision measurement system. *2010 2nd IEEE International Conference on Information Management and Engineering*, 55–60. <https://doi.org/10.1109/icime.2010.5477600>
- [15] Berkovic, G., & Shafir, E. (2012). Optical methods for distance and displacement measurements. *Advances in Optics and Photonics*, 4(4), 441. <https://doi.org/10.1364/aop.4.000441>
- [16] Grgec Bermanec, L., Katic, M., & Zvizdic, D. (2019). Characterization of gas pressure balances at LPM. *Measurement*, 136, 689–693. <https://doi.org/10.1016/j.measurement.2018.10.070>
- [17] Grgec Bermanec, L., Zvizdic, D., & Simunovic, V. (2014). Development of Method for Determination of Pressure Balance Piston fall Rate. *ACTA IMEKO*, 3(2), 44. https://doi.org/10.21014/acta_imeko.v3i2.105
- [18] Kobata, T. (2011). Multiple cross-float system for calibrating pressure balances. *PTB Mitteilungen*, 121(3), 274–277.
- [19] Vámosy13, W., & Koçaş1, I. (2011). Evaluation of cross-float measurements with pressure balances—Results of EURAMET project. *PTB-Mitteilungen*, 121(3), 295.
- [20] Hong, B., Pan, Z., Gu, S., & Zhang, Z. (2018). An Investigation of the High Pressure Controlled clearance Dead weight Piston Gauge. *2018 5th International Conference on Systems and Informatics (ICSAI)*, 734–738. <https://doi.org/10.1109/icsai.2018.8599365>
- [21] Muset, B., & Emerich, S. (2012). Distance measuring using accelerometer and gyroscope sensors. *Carpathian Journal of Electronic and Computer Engineering*, 5, 83–86. https://ieec.utcluj.ro/cjece/web/CJECE_VOL5_2012/17_Muset.pdf



Adam Brzozowski Deputy Director of the Department of Mechanics and Acoustics for Pressure and Flow at the Central Office of Measures, PhD student in an implementation doctorate program at the Warsaw University of Technology. Specializes in metrology, calibration and measurement methods, uncertainty budget, particularly in the field of pressure and dynamic pressure.



Piotr Gazda Assistant professor at the Department of Sensors and Measurement Systems, Institute of Metrology and Biomedical Engineering, Warsaw University of Technology. In his scientific work, he deals with the development of measurement methods and innovative research stations, especially in the field of magnetoelectric phenomena. He also conducts research on the use of artificial intelligence in

measurement systems.



Roman Szewczyk is a longtime employee of LUKASIEWICZ Research Network – Industrial Research Institute for Automation and Measurements PIAP. Specialized in stochastic optimization, symbolic regression and artificial neural networks for regression models. The Member of the Metrology Council appointed by the Minister of Development and Technology (2022–2027). The Member (2015–2023) and

Deputy of the Chairman (2015–2018) of 14. Workgroup on Sensors (including biosensors) and intelligent sensor networks in the Ministry of Economy as a part of the Operational Programme Intelligent Development. The Chairman of 2. Workgroup on Digital Support for Industry in a Team for Industrial Transformation, the Ministry of Development (2016–2017). Coordinator of research project „Customizable cyber-physical system for distributed monitoring and control in agriculture” elaborated in bilateral cooperation with Israel (2018).



Michal Nowicki Senior Research Fellow at Department of Mechatronics, Robotics and Digital Manufacturing, Faculty of Mechanics, Vilnius Gediminas Technical University. He specializes in the design and construction of experimental measurement systems, in particular magnetic and magnetomechanical ones, and the development of new sensor structures. Privately, he is interested in

technical archeology and exotic technologies.